P H Y S I C A L   R E V I E W   L E T T E R S

Plasmon-Assisted Two-Slit Transmission: Young's Experiment Revisited

H. F. Schouten,[1] N. Kuzmin,[2] G. Dubois,[2] T. D. Visser,[1] G. Gbur,[3] P. F. A. Alkemade,[4] H. Blok,[5] G. W. 't Hooft,[2,6] D. Lenstra,[1,7] and E. R. Eliel[2,*]

[1]*Department of Physics and Astronomy, Free University, De Boelelaan 1081, 1081 HV Amsterdam, The Netherlands*
[2]*Huygens Laboratory, Leiden University, P.O. Box 9504, 2300 RA Leiden, The Netherlands*
[3]*Department of Physics & Optical Science, UNC Charlotte, 9201 University City Boulevard, Charlotte, NC 29223, USA*
[4]*Kavli Institute of Nanoscience, Applied Physics, Delft University of Technology, Lorentzweg 1, 2628 CJ, Delft, The Netherlands*
[5]*Department of Electrical Engineering, Delft University of Technology, Mekelweg 4, 2628 CD Delft, The Netherlands*
[6]*Philips Research Laboratories, Prof. Holstlaan 4, 5656 AA Eindhoven, The Netherlands*
[7]*COBRA Research Institute, Eindhoven Univerity of Technology, P.O. Box 513, 5600 MB Eindhoven, The Netherlands*
(Received 24 September 2004; published 7 February 2005)

We present an experimental and theoretical study of the optical transmission of a thin metal screen perforated by two subwavelength slits, separated by many optical wavelengths. The total intensity of the far-field double-slit pattern is shown to be reduced or enhanced as a function of the wavelength of the incident light beam. This modulation is attributed to an interference phenomenon at each of the slits, instead of at the detector. The interference arises as a consequence of the excitation of surface plasmons propagating from one slit to the other.

Recently, there has been a surge of interest in the phenomenon of light transmission through subwavelength apertures in metal plates. This followed the observation by Ebbesen *et al.* [1] that the transmission through a two-dimensional hole array can be much larger than predicted by conventional diffraction theory [2]. This discovery has rekindled the interest in a similar but simpler problem, viz., the transmission of a one-dimensional array of subwavelength *slits* in a metal film, i.e., of a metal grating [1,3–16]. In many cases the enhanced transmission of hole or slit arrays has been explained in terms of the excitation of (coupled) surface plasmons on the metal film [3–6], an explanation that has recently been challenged [16]. It has been shown that, for slit arrays, Fabry-Pérot-type waveguide resonances can also give rise to a considerably enhanced transmission [5,7,9,10,12].

In the present Letter we study an even more fundamental system than the metallic grating, namely, a thin metal layer perforated by just *two* parallel subwavelength slits. In contrast to the systems that have recently attracted so much attention, our slits are separated by *many* optical wavelengths. Thus we study the light transmission of a setup that lies at the heart of wave physics, namely, that of Thomas Young. We do, however, not focus on the well-known interference pattern named after him, but on the angle-integrated power transmission coefficient of the perforated screen, i.e., the transmission integrated over many interference orders. We show that this transmission coefficient is strongly modulated as a function of the wavelength of the incident light for the case that that light is TM-polarized, i.e., with the electric field aligned perpendicular to the slits. In contrast, there is no such modulation when the incident light is TE-polarized, or when the "wrong" metal is chosen. All our observations can be explained in

terms of a model involving the coherent transport of electromagnetic energy between the slits by surface plasmons.

Our samples consist of a 200 nm thick gold film, evaporated on top of a 0.5 mm thick fused quartz substrate with a 10 nm thick titanium adhesion layer between the gold and the glass. In such a sample a two-slit pattern is written using a focussed ion beam, each slit being 50 μm long and 0.2 μm wide. The slits are separated by a distance, as measured with a scanning electron microscope, of 4.9, 9.9, 14.8, 19.8, or 24.5 μm, respectively. Such a two-slit pattern, with the metallized side facing the laser, is illuminated at normal incidence with the well-collimated output beam (≈ 2 mm diameter) of a narrow-band cw Ti:sapphire laser, tunable between 740 and 830 nm. We detect in transmission, integrating the double-slit pattern (shown at the top of Fig. 1) over a large number of interference orders. The zeroth order peak is considerably stronger than the other orders because of non-negligible leakage through the bulk metal, and is therefore blocked by an opaque screen. The polarization of the incident light is either parallel (TE) or perpendicular (TM) to the long axis of the slits.

The results for the case of TM polarization are shown in Fig. 1. The transmission is seen to be approximately sinusoidally modulated as a function of wave number, the modulation period being inversely proportional to the slit separation. The visibility $\mathcal{V}$ of the fringes is of order 0.2, roughly independent of the slit separation. Note that the fringes are superposed on an offset that gradually increases as a function of wave number.

In contrast, for a TE-polarized incident beam the detected signal shows no modulation whatsoever (see bottom frame of Fig. 1). Equally, no modulation is observed when the experiment is performed using a 200 nm thick titanium
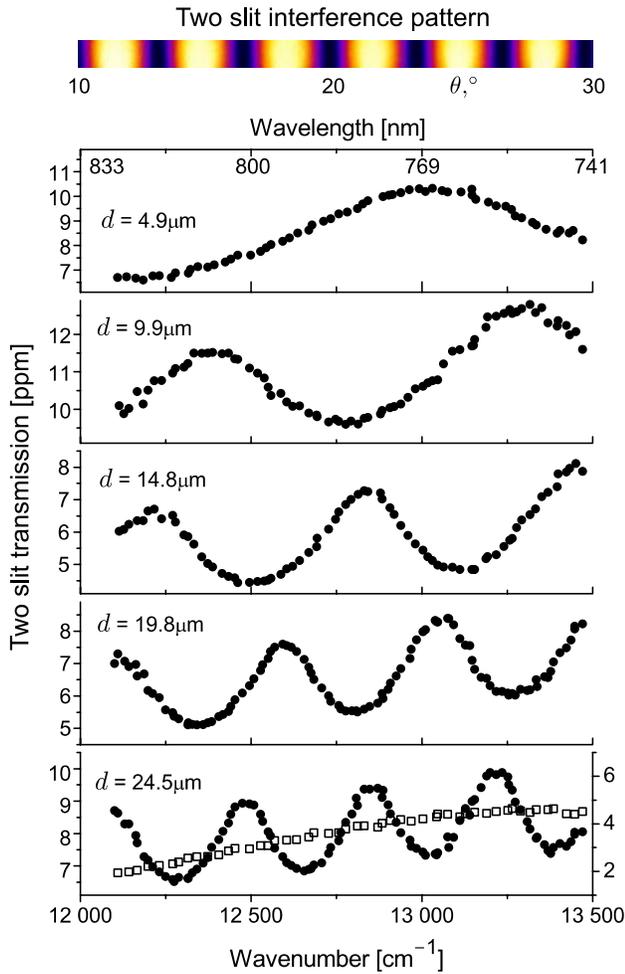
FIG. 1 (color online).   The frame at the top shows the Young-type interference pattern behind the screen, as recorded with a charge coupled device camera. The other frames display experimental transmission spectra for a TM-polarized input beam (polarization perpendicular to the long axis of the 200 nm wide slits), recorded by integrating over the interference pattern. The value of the slit separation d is indicated in each of the frames. In the frame at the bottom ($d = 24.5$ μm) the results for TE-polarized incident light (open squares) are included; the scale at the right applies to this choice of polarization.

layer instead of gold, independent of the polarization of the incident radiation.

The observed strong polarization anisotropy and the dependence on the screen material both suggest that *surface plasmons* propagating along the gold-air interface lie at the heart of the observed phenomena. Explanations in terms of waveguide modes within the slit [5,7,9,10,12] or diffractive evanescent waves [16] are excluded by the observed *dependence* of the spectral modulation period and the *independence* of the modulation depth on the slit separation.

The propagation constant k_{sp} of a surface plasmon is given by [17]

$$k_{sp} = k_0 \sqrt{\frac{\varepsilon_m \varepsilon_d}{\varepsilon_m + \varepsilon_d}}, \qquad (1)$$

where ε_m and ε_d are the complex (relative) dielectric constants of the metal and dielectric, respectively, and $k_0 = 2\pi/\lambda_0$ the free-space wave number. The surface-plasmon wavelength is related to the real part of k_{sp} by $\lambda_{sp} = 2\pi/\mathrm{Re}(k_{sp}) \equiv \lambda_0/n_{sp}$, while its (amplitude) decay length is given by $1/\mathrm{Im}(k_{sp})$. For the gold-air interface at $\lambda_0 = 800$ nm, $n_{sp} = 1.02$ and $1/\mathrm{Im}(k_{sp}) \approx 80$ μm [18], considerably larger than the separation of any pair of slits. Consequently, surface plasmons propagating along this interface can easily cover the distance between the slits. In contrast, the amplitude decay length for the Ti-air interface at $\lambda_0 = 800$ nm is only ≈ 7 μm [19], considerably shorter than the separation of most of our double slits. Surface plasmons propagating along this interface decay over too short a length, as is confirmed by our experiments.

Since the gold film is sandwiched between glass ($\varepsilon_d \approx 2.1$) and air ($\varepsilon_d = 1$), the surface plasmons living on the Au-air and Au-glass interfaces have different (complex) propagation constants [see Eq. (1)]. Moreover, a 10 nm film of Ti lies between the glass substrate and the gold film, resulting in a much reduced decay length of the surface plasmons on that interface. Consequently, of all the interfaces that we probe in the experiment, only the Au-air variety supports surface plasmons propagating over distances comparable to the separation of the slits.

The function of the slits in our experiment is threefold. First, the slits transmit part of the incident radiation, together giving rise to a conventional Young-type interference pattern. Second, each slit scatters part of the incident radiation into a plasmonic channel, bridging the momentum gap between the surface plasmon and free-space radiation. Third, each slit provides a mechanism for back-converting a surface plasmon into free-space radiation.

When the incident light is TM-polarized the surface plasmon that is excited at one of the slits propagates towards its partner slit. There it is partially back-converted into light (see Fig. 2). The plasmon-mediated amplitude at this slit interferes with the amplitude of the light that is directly transmitted by that slit. Because of the subwavelength nature of our slits these two contributions are of comparable magnitude.

FIG. 2.   Two interfering paths leading to light emission from the slit at the left. A similar set of paths gives rise to emission from the slit on the right. The dashed line indicates the propagating surface plasmon.

The field amplitude at the second slit's unilluminated side can now be written as

$$E_{\text{slit}}^{(2)} = E_0(\lambda_0)[1 + \beta(k_{\text{sp}}) \exp(i(k_{\text{sp}}d + \Phi))], \quad (2)$$

where d is the slit separation, $\beta(k_{\text{sp}})$ the relative strength of the plasmon contribution, and Φ a phase factor associated with the scattering and back-conversion processes. The field amplitude $E_{\text{slit}}^{(2)}$ behind the second slit is thus enhanced or suppressed, depending on the argument of the complex phase factor in Eq. (2). Because our laser beam is normally incident on the sample and symmetrically illuminates the two slits, the field amplitude behind the first slit is given by $E_{\text{slit}}^{(1)} = E_{\text{slit}}^{(2)}$.

In the present experiment the far-field two-slit pattern arises as a consequence of the interference of *four* paths, two of which are partially plasmonic, while the other two are photonic all the way. Although the number of interfering channels is four in the present experiment, the far-field pattern that arises behind the sample is simply that of Young's experiment, i.e., a pattern of *two* interfering sources. The novel aspect is that the strength of each of these sources is enhanced or reduced due to the interference of a photonic and a plasmonic channel.

We collect a large number of interference orders on our detector thereby effectively erasing the far-field two-slit pattern. Hence, the signal S, picked up by our detector, is simply proportional to the total power radiated into the acceptance angle of the detector, i.e., to twice the power radiated by each slit separately,

$$S \propto 2E_0^2(\lambda_0)[1 + \beta^2(k_{\text{sp}}) + 2\beta(k_{\text{sp}})\cos(k_{\text{sp}}d + \Phi)]. \quad (3)$$

From the experiment we extract that, across the wavelength range probed, the parameter $\beta(k_{\text{sp}}) \approx 0.1$. Further, in order to reliably fit our experimental transmission spectra with the expression given by Eq. (3) and the measured values for the slit separation we need to take the dispersion of the surface plasmon's propagation constant into account. This provides additional support for our claim that the effect observed here is to be attributed to communication between the slits by propagating surface plasmons. Regretfully, we cannot extract a value for the phase factor Φ from the experimental data because the magnitude of $k_{\text{sp}}d$ is not known with sufficient accuracy.

The model outlined above suggests that the spectrum of the angular-integrated intensity shows a structure identical to that of Fig. 1 when one of the two slits is covered by an opaque screen at the *nonilluminated* side of the sample. The signal S on the detector has half the value as given in Eq. (3). However, when the opaque screen is positioned at the *illuminated* side, we predict that the spectrum of the angular-integrated intensity will be structureless. In this case the signal is given by $S \propto E_0^2(\lambda_0)[1 + \beta^2(k_{\text{sp}})]$.

Surface plasmons can also be excited when the incident light is TE-polarized, in this case at the sub-μm top and bottom edges of the 50 μm long slits. These surface excitations do not effectively couple to the other slit, being predominantly emitted in the wrong direction. In the absence of plasmon-mediated interslit coupling, the angular-integrated double-slit spectrum is expected to be smooth, and this is in line with our experimental findings (see Fig. 1). Note that for this polarization the incident light is beyond cutoff for each slit separately.

Theoretically, we calculate the transmission of the double-slit system using a rigorous scattering model based on a Green's function approach [20,21]. The transmission coefficient is normalized on the geometrical optical transmission through the two slits [21]. The wavelength dependence of the dielectric constant of the gold film is fully taken into account [18].

In Fig. 3 the total transmission of the two-slit configuration is shown as a function of the wavelength of the incident radiation. When the incident field is TE-polarized, the transmission of the double slit is small and weakly modulated as a function of wavelength. In contrast, for a TM-polarized incident field, the transmission shows a strong modulation as a function of wavelength with a visibility $\mathcal{V}_{\text{theor}} \approx 0.45$. Overall, the agreement between the experiment and the results of the Green's function model is seen to be good, the theoretical data having a somewhat larger visibility than the experimental ones ($\mathcal{V}_{\text{exp}} \approx 0.2$). This difference can be attributed to the different embedding of the gold film in the experiment and in the calculation. While in the experiment the gold film is asymmetrically encapsulated, in the calculation the materials at either side of the film are identical, greatly enhancing the plasmonic effects.

Using the theoretical model outlined above we have also calculated the intensity distribution, i.e., the value of $|E|^2$, on both sides of a freestanding perforated gold film (see Fig. 4). For calculational convenience we have taken values of the slit separation that are considerably smaller than those of the experiment, viz. $5\lambda_{\text{sp}}/2$, where the transmission is maximum, and $4\lambda_{\text{sp}}/2$, where the transmission is minimum. In the first case (maximum transmission) one
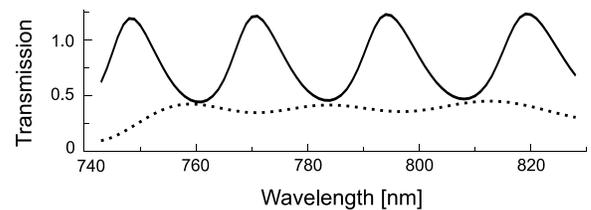

FIG. 3. The calculated angular-integrated transmission coefficient of a double slit in a 200 nm thick gold film as a function of the wavelength of the incident light. The slits are 200 nm wide and separated by 25.0 μm. The full line displays the results for TM polarization, while the dotted line (magnified 10 times) shows the results for the case of TE polarization. The transmission coefficient is normalized to the area of the slits.
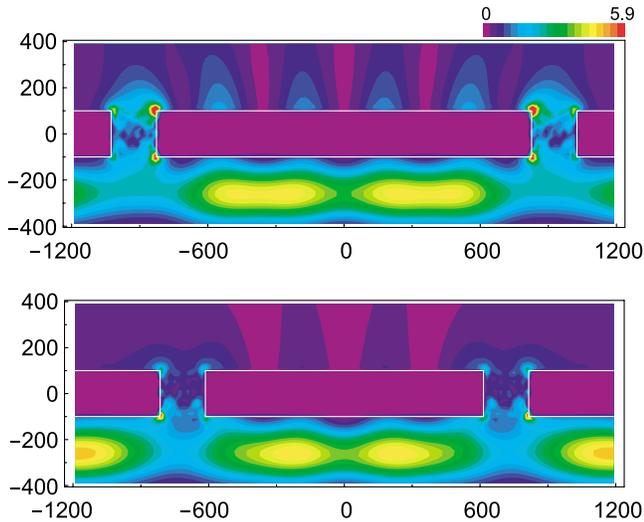
FIG. 4 (color online). Intensity distribution in the immediate vicinity of the double-slit system for TM-polarized incident radiation when the transmission is maximum (top frame, slit separation equal to $5\lambda_{sp}/2$), and minimum (bottom frame, slit separation equal to $4\lambda_{sp}/2$). The field is incident from below. All lengths are in nm.

can distinguish at the dark side of the metal film a well-developed standing-wave pattern along the interface, having six antinodes, two of which coincide with the slits themselves. In contrast, when the transmission is minimum the antinodes of the standing-wave pattern do not coincide with the slits; at these locations one rather finds a node of the standing-wave pattern. In both cases the intensity is seen to rapidly decay away from the air-metal interface. These results also allow us to determine the value of the phase Φ, introduced in Eq. (2), and we find $\Phi \approx \pi$.

In this Letter we have shown that Young's double-slit experiment, often seen as proof of the wave nature of light, can provide powerful evidence for the role of propagating surface plasmons in the transmission of perforated metal screens. The transport of electromagnetic energy by the surface plasmons over distances of many optical wavelengths gives rise to an interference phenomenon in the slits that enhances or reduces the intensity of the far-field pattern.

*Electronic address: eliel@molphys.leidenuniv.nl

[1] T. W. Ebbesen, H. J. Lezec, H. F. Ghaemi, T. Thio, and P. A. Wolff, Nature (London) **391**, 667 (1998).
[2] H. A. Bethe, Phys. Rev. **66**, 163 (1944).
[3] U. Schröter and D. Heitmann, Phys. Rev. B **58**, 15419 (1998).
[4] M. B. Sobnack, W. C. Tan, N. P. Wanstall, T. W. Preist, and J. R. Sambles, Phys. Rev. Lett. **80**, 5667 (1998).
[5] J. A. Porto, F. J. García-Vidal, and J. B. Pendry, Phys. Rev. Lett. **83**, 2845 (1999).
[6] H. E. Went, A. P. Hibbins, J. R. Sambles, C. R. Lawrence, and A. P. Crick, Appl. Phys. Lett. **77**, 2789 (2000).
[7] S. Astilean, P. Lalanne, and M. Palamaru, Opt. Commun. **175**, 265 (2000).
[8] Y. Takakura, Phys. Rev. Lett. **86**, 5601 (2001).
[9] M. M. J. Treacy, Phys. Rev. B **66**, 195105 (2002).
[10] Q. Cao and P. Lalanne, Phys. Rev. Lett. **88**, 057403 (2002).
[11] P. Lalanne, C. Sauvan, J. P. Hugonin, J. C. Rodier, and P. Chavel, Phys. Rev. B **68**, 125404 (2003).
[12] A. Barbara, P. Quémerais, E. Bustarret, T. López-Rios, and T. Fournier, Eur. Phys. J. D **23**, 143 (2003).
[13] J. R. Suckling, A. P. Hibbins, M. J. Lockyear, T. W. Preist, J. R. Sambles, and C. R. Lawrence, Phys. Rev. Lett. **92**, 147401 (2004).
[14] F. J. García-Vidal, H. J. Lezec, T. W. Ebbesen, and L. Martín-Moreno, Phys. Rev. Lett. **90**, 213901 (2003).
[15] A. P. Hibbins, J. R. Sambles, C. R. Lawrence, and J. R. Brown, Phys. Rev. Lett. **92**, 143904 (2004).
[16] H. J. Lezec and T. Thio, Opt. Express **12**, 3629 (2004).
[17] H. Raether, *Surface Plasmons on Smooth and Rough Surfaces and on Gratings* (Springer, Berlin, 1988).
[18] *Handbook of Optical Constants of Solids*, edited by E. D. Palik (Academic Press, Boston, 1985).
[19] P. B. Johnson and R. W. Christy, Phys. Rev. B **9**, 5056 (1974).
[20] T. D. Visser, H. Blok, and D. Lenstra, IEEE J. Quantum Electron. **35**, 240 (1999).
[21] H. F. Schouten, T. D. Visser, D. Lenstra, and H. Blok, Phys. Rev. E **67**, 036608 (2003).